*Biomedical Research 2017; 28 (5): 2262-2266* *ISSN 0970-938X*
*www.biomedres.info*

# *In-vitro* cytotoxicity of biosynthesized Zinc oxide nanoparticles towards cardiac cell lines of *Catla catla.*

**Wei Ji, Diqi Zhu, Yiwei Chen, Jingjing Hu, Fen Li***

Department of Cardiology, Shanghai Children's Medical Center, Shanghai Jiao Tong University School of Medicine, Shanghai, PR China

## Abstract

**Objective: The present report describes the green synthesis of Zinc oxide nanoparticles (ZnO NPs) using *Argemone maxicana* leaf extract by an eco-friendly approach. Also, the *in-vitro* cytotoxicity of prepared ZnO NPs against the cardiac cell lines of Sahul India *Catla catla* fish (SICH) was studied.**

**Methods: ZnO NPs were prepared by using *Argemone maxicana* leaf extract as reducing and stabilizing agent. The synthesized ZnO NPs have been characterized by using techniques such as FT-IR, XRD, UV-Vis, Photo luminescence, EDS and SEM instruments. Also, the *in-vitro* cytotoxicity of the synthesized ZnO NPs was tested against the SICH cell lines.**

**Results: The synthesized ZnO NPs were analysed using different characterization techniques. XRD and SEM have confirmed the cubic structure of the prepared ZnO NPs with crystalline nature. FTIR showed the capping of plant biomolecules onto the surface of ZnO NPs. The *in-vitro* cytotoxicity of *Argemone maxicana* extract mediated ZnO NPs showed the concentration dependant cytotoxicity against SICH cell lines.**

**Conclusions: A simple, fast and environment friendly approach for the preparation of ZnO NPs using *Argemone maxicana* leaf extract is showed in this work. *Argemone maxicana* extract mediated ZnO NPs have showed the concentration dependant cytotoxicity against SICH cell lines.**

**Keywords:** ZnO NPs, *Argemone maxicana* leaf, *In-vitro* cytotoxicity, SICH cell lines.

*Accepted on October 26, 2016*

## Introduction

Zinc oxide nanoparticles (ZnO NPs) are considered as a unique and key nano material. They have attracted wide-ranging research due to their distinguishing properties and their new applications in the fields of nanoscience and technology. ZnO NPs has numerous properties like piezoelectric, pyroelectric, semiconducting, optoelectronics and catalysis [1]. ZnO is an n-type semiconductor with and high band gap energy of 3.37 eV and a large exciton binding energy of 60 meV. Due to their high surface-to-volume ratio, ZnO NPs have gained various chemical and physical properties. ZnO NPs can be prepared by several approaches, which includes the chemical vapor deposition [2], hydrothermal synthesis [3], vapor-liquid-solid (VLS) [4], zinc oxidation [5], vapor phase deposition [6] and metallorganic chemical vapor deposition [7] respectively. Among these methods, vapor-liquid-solid and hydrothermal synthesis are the widely used for preparing ZnO NPs. In recent times, biosynthesis of nanomaterials was achieved by using plant extracts, natural biomolecules and microorganisms because of their cheap, non-hazardous, eco-friendly and biodegradable nature. On the other hand, the dispensability of ZnO NPs can be improved by surface stabilizing agents, which can be easily achieved by green synthetic approaches. Several eco-friendly methods have been used for the preparation of ZnO NPs [8]. For instance, extract of Aloe barbadensis Miller leaf is already been reported for the preparation of water dispersible ZnO NPs [9]. In the present work, *Argemone maxicana* plant extract have used for the ZnO NPs synthesis using green chemistry principles. It is well known that the plant extracts play key role in the synthesis various nanomaterials such as silver nanoparticles [10], graphene [11,12] etc. The bioconstituents that are present in the *Argemone maxicana* extract are mainly responsible for reduce of Zinc nitrate to ZnO NPs. Further, the *in-vitro* cytotoxicity of the prepared ZnO NPs against the cardiac cell lines of *Catla catla* was studied.

## Experimental Section

### *Materials*

Zinc nitrate hexahydrate ($Zn(NO_3)_2 \bullet 6H_2O$), Bovine serum albumin (BSA), Dimethyl sulfoxide (DMSO) were obtained from Sigma-Aldrich chemicals Ltd.

### *Preparation of Argemone maxicana extract*

*Argemone maxicana* plant leaves were washed with double distilled water to remove the dust particles and dried under

sunlight. About 20 g of cleaned and dried leaves were finely cut into powder and boiled in 100 mL of distilled water for about 40 min. The obtained extract solution was then cooled down to room temperature and filtered through cellulose nitrate membrane to obtain clear extract solution. The obtained extract was then stored in refrigerator for future experiments.

### *Synthesis of ZnO NPs*

For the synthesis of NPs, 50 mL of *Argemone maxicana* leaves extract was taken and boiled at 60-80°C by using a stirrer-heater. Then, 5 g of zinc nitrate was added to the solution as the temperatures reached at 60°C. This mixture was then heated to obtain a deep yellow colored suspension. This paste was then collected in a ceramic crucible and kept for heating in a furnace for about 2 h at 400°C. A light white colored powder was obtained and used for future characterizations and cytotoxicity studies. The material was powdered using a mortar and pestle so, that got a fine powder, which is easy for further characterizations.

### *Cytotoxicity evaluation*

The Sahul India *Catla catla* fish heart cell lines (SICH) were maintained in Leibovitz'sL-15 medium at 28°C and pH 7.0-7.4, supplemented with 2 mM L-glutamine, streptomycin 100 µg/mL, penicillin 100 IU/mL and 10% fetal bovine serum (FBS). Later, the cells were sub-cultured by following a standard procedure for about every two to three days. Actively growing cells were harvested in exponential growth phase and diluted to $10^5$ cells/mL in Leibovitz'sL-15 medium. Then the cells were shaken for mixing and added to each well in 96-well tissue culture plate at the concentration of $2 \times 10^4$ cells/well which followed by incubation at 28°C for over night. The supernatant in all the wells was trowed followed by the addition of medium containing 3, 6, 9, 18 and 36 µg/mL of $Zn(NO_3)_2 \cdot 6H_2O$ and ZnO NPs and left for 24 h for cell viability analysis. On the other hand a control experiment was performed without zinc salt and ZnO NPs.

### *MTT assay*

MTT assay was conducted to know about the percentage viability of cells. After the exposure of ZnO NPs for 24 h to the cells, the medium was trowed out and 20 µL of MTT reagent in PBS (5 mg/mL) was added followed by incubation for 4 h at 20°C. The solution was then carefully removed, and the cells were rinsed with PBS buffer for two times. Later, DMSO (150 µL/well) was added to cells and each well was measured for their optical density at 490 nm.

### *Characterization*

A D8-Advanced, Bruker diffractometer was used to obtain the XRD pattern of the obtained ZnO NPs from 20° to 70° in 2θ with Cu Kα (λ=0.1546 nm) radiation. Optical absorption of ZnO NPs was obtained by using a UV-vis (Perkin Elmer Lambda 950) spectrophotometer. A JASCO-FT-IR instrument was used to know about the surface capping of the obtained ZnO NPs. Additionally, the morphology, size of the ZnO NPs sample was characterized by using LEO 1530FEGSEM Scanning Electron Microscopy instrument. A simultaneous measurement of chemical composition was analysed using BRUKER INDIA energy dispersive spectroscopy instrument. Photoluminiscent spectrum for the prepared ZnO NPs was analysed by using Hitachi fluorescent spectroscopy instrument.

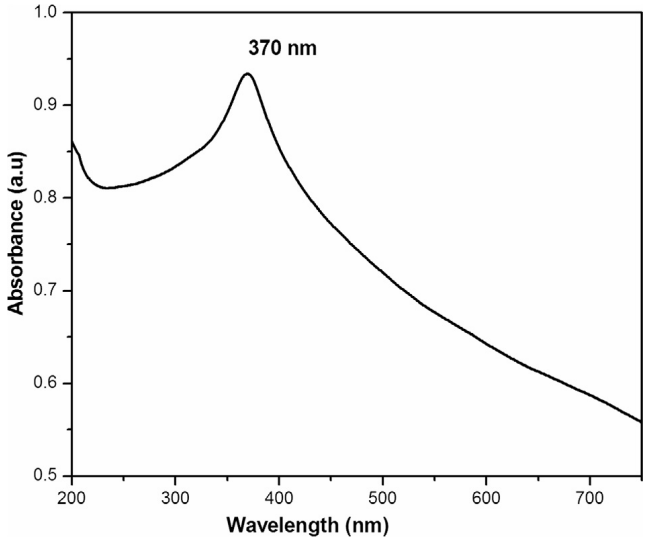


***Figure 1.*** *UV-visible spectrum of biosynthesized ZnO NPs.*

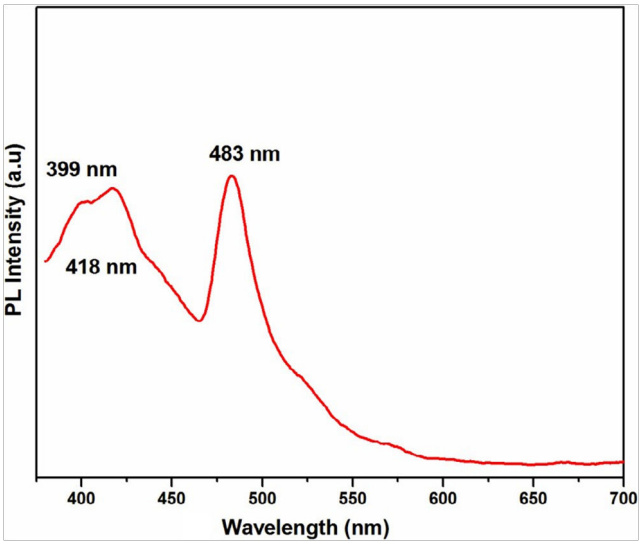


***Figure 2.*** *PL spectrum of ZnO NPs.*

## Results

Figure 1 showed the optical absorbance spectrum of the *Argemone maxicana* plant extract mediated ZnO NPs with an absorbance at 370 nm, indicating the formation of ZnO NPs. The formation of ZnO NPs is also visually confirmed by the change of color of the solution to deep yellow. Figure 2 showed the PL spectrum of ZnO NPs prepared by using leaf extract of *Argemone maxicana*. PL spectrum showed the existence of the peak at 399 nm characteristic to the emission in UV region. On the other hand, the peak present at 418 nm is due to the defect corresponding to UV emission. Similarly, the

peak existed at 483 nm is because of the strong blue-green band. The X-ray diffraction pattern exhibited the presence of peaks corresponding to ZnO NPs at 31.7°, 34.4°, 36.2°, 47.5°, 56.5°, 62.8°, 66.3°, 67.9°, 69.0°, 72.5 and 76.9° respectively with characteristic planes related to (100), (002), (101), (102), (110), (103), (200), (112), (201), (004), (202) correspondingly. These results also confirmed the wurtzite structure of synthesized ZnO NPs (shown in Figure 3). On the other hand, the crystallite size of the ZnO NPs is calculated using sherrer's formula and is found to be 24 nm.

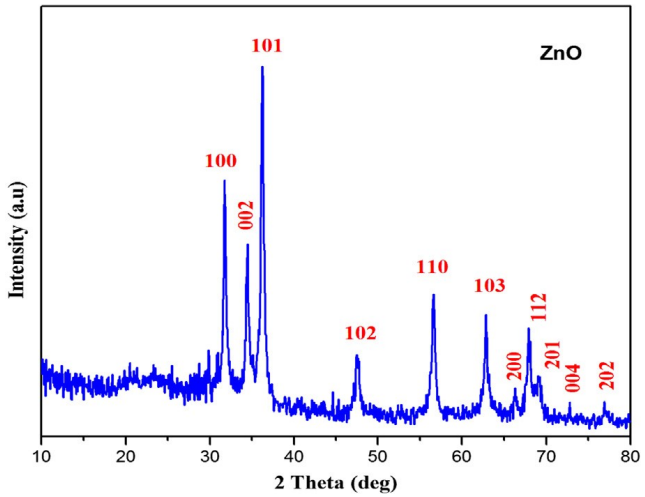


***Figure 3.*** *XRD patterns of ZnO NPs.*

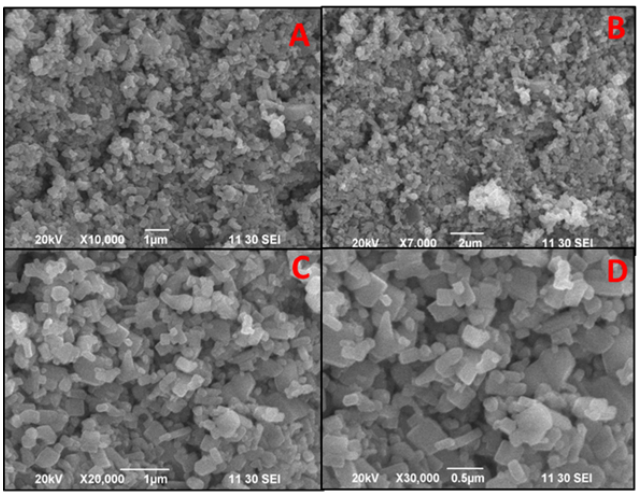


***Figure 4.*** *SEM images of ZnO NPs prepared using plant extract.*

Figure 4, showed the SEM images of ZnO NPs at different magnifications. From the figure, it can be seen that the obtained ZnO NPs are in the size range from 100-190 nm with cubic structure. Additionally, the EDS spectrum of ZnO NPs showed the presence of elemental peaks to corresponding to Zinc and Oxygen (Figure 5). Figure 6 represented the FT-IR spectra of ZnO NPs synthesized from aqueous leaf extract of *Argemone maxicana* plant by a biosynthesis approach. Figure showed the presence of absorption bands at 768, 710 and 849 $cm^{-1}$ corresponding to the aromatic C-H out of plane bending vibrations in a typical 1,2,3 tri-substituted benzene ring, mono substituted benzene ring and 1, 4 di-substituted benzene ring. The presence of band at 1029 $cm^{-1}$ is characteristic to C-N stretching vibrations of amine functional group [13]. On the other hand the absorption bands existed in the region 1411-1617 $cm^{-1}$ is related to aromatic ring vibrations. The two weak IR band absorptions in the region of 2900-2750 $cm^{-1}$ further indicated the existence of aromatic aldehydes [14]. Similarly, the weak absorption band present at 2049 $cm^{-1}$ is because of the C≡C vibrational stretching. The intense and broad band existed at 3237-3565 $cm^{-1}$ is corresponding to OH stretching vibrations. The absorption band at 450-540 $cm^{-1}$ indicated the presence of ZnO NPs.

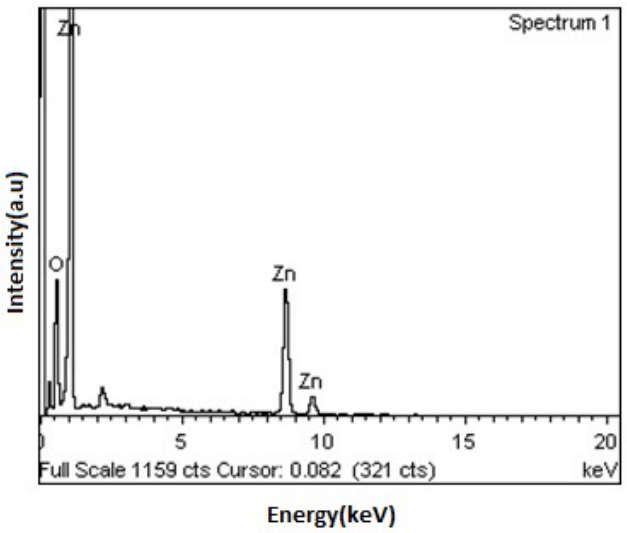


***Figure 5.*** *EDS spectrum of biosynthesized ZnO NPs.*

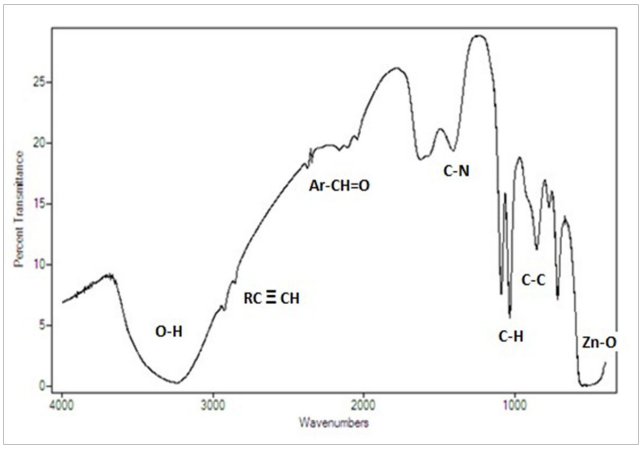


***Figure 6.*** *FTIR spectrum of biosynthesized ZnO NPs.*

An MTT test is conducted to investigate the percentage cell viability of SICH cells after exposing for about 24 h to Zinc salt and ZnO NPs of different concentrations. Figure 7 represented the *in-vitro* cytotoxicity of Zinc salt and ZnO NPs (ranging from 3 to 36 µg/mL) after their exposure to SICH cell lines. It is observed that zinc salt showed toxicity to SICH cell lines even at very low concentrations of about 3 µg. On the other hand, the same concentration of ZnO NPs is not comparatively toxic to the cell lines. On the other hand, a systematic increase in the cytotoxicity is found with a raise in

the Zinc salt and ZnO NPs concentration, suggesting that the cytotoxicity of the plant extract mediated ZnO NPs is dose dependent.

## Discussion

The initial formation of ZnO NPs was identified by visual color change of reaction mixture to deep yellow color during the synthesis. It is interesting to note that the reaction is completed in 3h at 60°C to 80 °C, which is comparatively less and faster than the previous reports [15-17]. UV-visible spectrum (Figure 1) showed the presence of absorbance peak at 370 nm, which is due to their large exciton binding energy at room temperature. The optical absorbance at 370 nm further confirmed the slight blue-shift in the absorbance when compared to that of bulk material (i.e. 377 nm). However, this slight blue shift in the optical absorbance may be due to the quantum confinement effect of nanoparticles. The PL spectra of ZnO NPs represented in Figure 2, showed the luminescent region between 418-483 nm, which is because of the various defects like the presence of interstitial Zn and also due to the existence of the donor and acceptor states in the region between the conduction and valence bands. On the other hand, the ZnO NPs also exhibit strong emission in visible region due to the deportment of open flaws, which may be due to the increased high surface to volume ratio with decrease in the size in case of ZnO NPs. This resulted in the formation of a large number of defects on the surface of ZnO NPs.

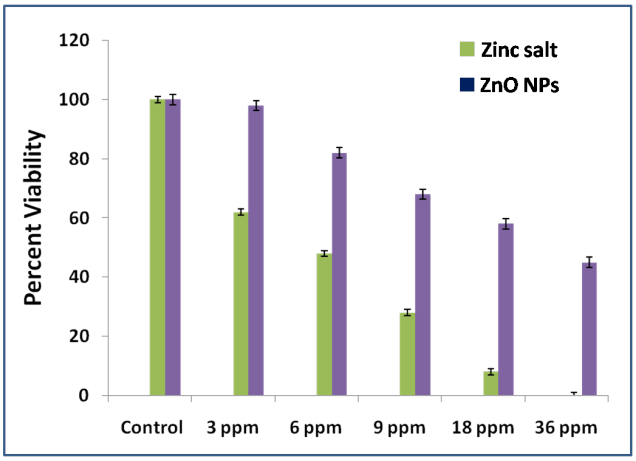


***Figure 7.*** *Cell viability of SICH cell lines induced by ZnO NPs.*

From the XRD pattern (Figure 3), it is found that all the peak intensity values were characteristics to the hexagonal wurtzite structure of the synthesized ZnO NPs. The narrow and stiff diffraction peaks showed in the XRD pattern further indicated the crystalline nature of the ZnO NPs. However, no other crystalline impurities and remarkable shift in the diffraction peaks are observed indicating the purity of the obtained product. On the other hand, the anisotropic growth in the ZnO NPs is confirmed by the presence of a relatively high intensity of (101) peak, which indicated the preferred orientation of the crystallites. Also, the XRD patterns showed the planes values which are in good agreement with JCPDS No: 89-7102 [18,19]. The formation of ZnO NPs by *Argemone maxicana* plant extract is also showed by EDS analysis. From Figure 5, it represented the presence of oxygen and zinc peaks confirmed the ZnO NPs formation. On the other hand, presence of no peaks corresponding to impurities further indicated the purity of the prepared ZnO NPs. FTIR spectrum gives information about the various functionalities present on surface of ZnO NPs (shown in Figure 6). From the FTIR spectrum the presence of absorption band in the region of 450-540cm$^{-1}$ confirmed the formation of ZnO NPs. On the other hand, the broad absorption bands in FTIR spectrum existed at 1614, 3237, 2900 cm$^{-1}$ indicated the presence of aldehydes, hydroxyl and amine functional groups on the surface of the prepared ZnO NPs [13,14]. Similarly, the vibrations corresponding to the aromatic ring further confirmed that plant biomolecules could increase the stabilization of ZnO NPs in the aqueous medium via capping. All these results confirmed the formation of ZnO NPs stabilized with *Argemone maxicana* plant extract biomolecules.

In the present work, we have also tested the *in-vitro* cytotoxicity of ZnO NPs of increased concentrations prepared by using *Argemone maxicana* plant extract, to know whether biosynthesized ZnO NPs can exhibit a toxic effect on SICH cell lines. The results that are obtained after exposing to ZnO NPs have demonstrated that the cytotoxicity of nano ZnO is dose-dependent. However, these results are similar to the previous reports with other noble metal NPs against cancer cell lines. For example, Sireesh babu et al. have reported the concentration dependant cytotoxicity of AuNPs against human lung and colon cancer cell lines [20]. In contrast, Johnston et al. have reported the non toxic nature of spherical gold NPs when compared to gold nano rods which are more toxic [21]. However, these results indicated the dependence of cytotoxicity of nanomaterials on morphology and functional groups that are present on the NPs surface. From the Figure 7, it is found that the cytotoxicity of the synthesized ZnO NPs is dose dependent. On the other hand, the comparatively less cytotoxicity of the biosynthesized ZnO NPs with that of Zinc salt may be due to the Argemone mexicana extract biomolecules that are coated on the surface of NPs, which further enhance the cell lines growth resulting their increased viability after exposure to ZnO NPs.

## Conclusions

A low-cost, simple and biosynthesis method for the ZnO NPs preparation using *Argemone maxicana* leaf extract is showed in this work. FTIR studies showed the decoration of plant extract biomolecules onto the surface of ZnO NPs. SEM and XRD studied revealed the formation of cubic ZnO NPs. Further, *Argemone maxicana* extract mediated ZnO NPs have showed the concentration dependant cytotoxicity against SICH cell lines.

## Acknowledgement

This study was supported by 1. National Science Foundation of China (Grant number 81470443); 2. Science and Technology

Commission of Shanghai Municipality (Grant number 14JC1404700).

## References

1. Anasa S, Rahul S, Babithaa KB, Mangalarajac RV, Ananthakumar S. Microwave accelerated synthesis of zinc oxide nanoplates and their enhanced photocatalytic activity under UV and solar illuminations. Appl Surf Sci 2015; 355: 98-103.
2. Hu Y, Zhang Y, Chang Y, Snyder RL, Wang ZL. Optimizing the Power Output of a ZnO Photocell by Piezopotential. ACS Nano 2010; 4: 4220-4224.
3. Baruwati B, Kishore Kumar D, Sunkara VM. Hydrothermal synthesis of highly crystalline ZnO nanoparticles: A competitive sensor for LPG and EtOH. Sensors and Actuators B: Chemical 2006; 119: 676-682.
4. Chen CH, Chang SJ, Chang SP, Li MJ, Chen IC, Hsueh TJ, Hsu AD, Hsu CL. Fabrication of a white-light-emitting diode by doping gallium into ZnO nanowire on a p-GaN substrate. J Phys Chem C 2010; 114: 12422-12426.
5. Hsueh TJ, Hsu CL. Fabrication of gas sensing devices with ZnO nanostructure by the low-temperature oxidation of zinc particles. Sens Actuators B Chem 2008; 131: 572-576.
6. Gao PX, Ding Y, Wang IL. Crystallographic Orientation-Aligned ZnO Nanorods Grown by a Tin Catalyst. Nano Lett 2003; 3: 1315-1320.
7. Yang JL, An SJ, Park WI, Yi GC, Choi W. Photocatalysis Using ZnO Thin Films and Nanoneedles Grown by Metal-Organic Chemical Vapor Deposition. Adv Mater 2004; 16: 1661-1664.
8. Sagar BR, Thorat PV. A Review on Preparation, Characterization and Application of Zinc Oxide (ZnO) Nanoparticles by Green Synthesis Method. Int J Emerg Technol Adv Eng 2015; 5: 521-524.
9. Sangeetha G, Rajeshwari S, Venckatesh R. Green synthesis of zinc oxide nanoparticles by aloe barbadensis miller leaf extract: Structure and optical properties. Materials Res Bullet 2011; 46: 2560-2566.
10. Kiran Kumar HA, Badal Kumar M, Mohan Kumar K, Sireesh babu M, Sai Kumar T, Pavithra M, Ghosh AR. Antimicrobial and antioxidant activities of Mimusops elengi seed extract mediated isotropic silver nanoparticles. Spectrochimica Acta Part A: Mol Biomol Spectroscopy 2014; 130: 13-18.
11. Sireesh Babu M, Badal Kumar M. Biofabrication of Reduced Graphene Oxide Nanosheets Using Terminalia bellirica Fruit Extract. Current Nanoscience 2015; 12: 94-102.
12. Sireesh Babu M, Badal Kumar M, Raviraj V, Poliraju K, Sreedhara Reddy P. Bioinspired reduced graphene oxide nanosheets using Terminalia chebula seeds extract. Spectrochimica Acta Part A: Mol Biomol Spectroscopy 2015; 145: 117-124.
13. Bhuiyan NI, Begum J, Sultana M. Chemical composition of leaf and seed essential oil of Corriandrum sativum L. Bangladesh J Pharmacol 2009; 4: 150-153.
14. Sathayavathi R, Balamuralikrishna M, Venugopalal Rao S, Narayana Rao D. Bio synthesis of silver Nanoparticles using Corriandrum sativum leaf extract and their application in non-linear optics. Adv Sci Lett 2010; 3: 3-6.
15. Jayaseelan C, Rahuman AA, Kirthi AV, Marimuthu S, Santhoshkumar T, Bagavan A, Gaurav K, Karthik L, Rao KVB. Novel microbial route to synthesize ZnO nanoparticles using Aeromonas hydrophila and their activity against pathogenic bacteria and fungi. Spectrochim Acta A 2012; 90: 78-84.
16. Abdul Salam H, Sivaraj R, Venckatesh R. Green synthesis and characterization of zinc oxide nanoparticles from Ocimum basilicum L. var. purpurascens Benth.-Lamiaceae leaf extract. Mater Lett 2014; 131: 16-18.
17. Singh G, Babele PK, Kumar A, Srivastava A, Sinha RP, Tyagi MB. Synthesis of ZnO nanoparticles using the cell extract of the cyanobacterium, Anabaena strain L31 and its conjugation with UV-B absorbing compound shinorine. J Photochem Photobiol Biol 2014; 138: 55-62.
18. Rajiv P, Rajeshwari S, Venckatesh R. Bio-Fabrication of zinc oxide nanoparticles using leaf extract of Parthenium hysterophorus L. and its size-dependent antifungal activity against plant fungal pathogens. Spectrochim Acta A 2013; 112: 384-387.
19. Nagarajan S, Kuppusamy KA. Extracellular synthesis of zinc oxide nanoparticle using seaweeds of gulf of Mannar. J Nanobiotechnol 2013; 11: 39.
20. Sireesh babu M, Badal Kumar M, Shivendu R, Nandita D. Diastase assisted green synthesis of sizecontrollable gold nanoparticles. RSC Adv 2015; 5: 26727-26733.
21. Johnston HJ, Hutchison G, Christensen FM, Peters S, Hankin S, Stone V. A review of the in vivo and in vitro toxicity of silver and gold particulates: particle attributes and biological mechanisms responsible for the observed toxicity. Crit Rev Toxicol 2010; 40: 328-346.

***Correspondence to**

Fen Li

Department of Cardiology

Shanghai Children's Medical Center

Shanghai Jiao Tong University School of Medicine

PR China